



ELSEVIER

Journal of Electron Spectroscopy and Related Phenomena 112 (2000) 9–29

JOURNAL OF
ELECTRON SPECTROSCOPY
and Related Phenomena

www.elsevier.nl/locate/elspec

Inner shell excitation spectroscopy of molecules using inelastic electron scattering

Adam P. Hitchcock*

Department of Chemistry and Brockhouse Institute for Materials Research, McMaster University, 1280 Main Street West, Hamilton, ON L8S 4M1, Canada

Received 21 March 2000; accepted 9 June 2000

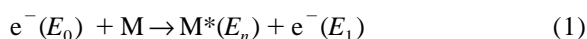
Abstract

Instrumentation and recent applications of inner-shell electron energy loss spectroscopy of gas phase molecules are reviewed. An overview of recent work in an historical perspective is provided. Comparison is made to the complementary technique of X-ray absorption spectroscopy. Highlights are described of recent applications in: polymer analogue studies, in situ studies of transient species, non-dipole spectroscopy, and systematic measurements of generalized oscillator strengths. © 2000 Elsevier Science B.V. All rights reserved.

1. Introduction

In electron energy loss spectroscopy (EELS) [1–5], a mono-energetic beam of electrons of incident energy E_0 is inelastically scattered in single collisions with an atom or molecule in a field-free region. The energy and angular distribution of the inelastically scattered electrons gives detailed spectroscopic information about the excited states of the target. Electronic excitation of the inner shell electronic levels of gaseous molecules is the subject of this review.

The basic electron energy loss process can be represented as:



where E_0 is the energy of the incident electron which

departs the collision with a residual energy of E_1 after exciting a target molecule (M) from the ground state to an excited state of energy E_n where $E_n = E_0 - E_1$, is the energy loss.

Momentum as well as energy is conserved. If one ignores the momentum of the molecular species, which is much heavier than the electron, the momentum transfer in the collision is:

$$\underline{K} = \underline{k}_0 - \underline{k}_1 \quad (2a)$$

$$K^2 = |\underline{K}|^2 = |\underline{k}_0 - \underline{k}_1|^2 = k_0^2 + k_1^2 - 2k_0k_1 \cos \theta \quad (2b)$$

where \underline{k}_0 is the wavevector of the incident electron with momentum $|\underline{k}_0|$, \underline{k}_1 is the wavevector of the outgoing electron scattered through an angle θ with momentum $|\underline{k}_1|$, and \underline{K} is the resultant momentum transfer. Varying the momentum transfer by changing impact energy and or scattering angle provides a means to vary the selection rules and thus to be able to excite from the ground state to excited states of different symmetries.

*Corresponding author. Tel.: +1-905-525-9140 ext. 24749; fax: +1-905-521-2773.

E-mail address: aph@mcmaster.ca (A.P. Hitchcock).

Single photon photoabsorption involving inner-shell electronic excitation is called near edge X-ray absorption fine structure spectroscopy (NEXAFS). NEXAFS is limited to studies of states which can be accessed from the ground state via electric dipole transitions. In contrast, EELS can provide a more complete investigation of atomic and molecular electronic structure. When the incident electron is fast (E_0 is large relative to the velocity of the target electron which gets excited) and it is scattered through a small angle, the momentum transferred to the target from the colliding electron is very small, the interaction between this electron and the target is weak, and electric dipole processes dominate. There is a simple quantitative relation between the dipole-regime energy loss and photoabsorption spectra. When the scattering angle becomes large (typically $> 10^\circ$), the momentum transferred from the incident electron into the target increases. This results in relaxation of the electric-dipole selection rules, resulting in excitation of higher order electric multipole transitions. If the impact energy is reduced to values only slightly higher than the transition energy — so-called near-threshold conditions — then spin-forbidden electronic transitions can be excited with significant probability on account of the exchange interaction of the incident and target electrons.

This article deals with the application of electron energy loss spectroscopy to studies of dipole and non-dipole inner-shell (core) electronic excitation, a subset of EELS which is distinguished with the acronym ISEELS. The goals are to provide a reasonable overview of the technique — its historical development, and current capabilities; to illustrate those capabilities using examples from my laboratory, and to discuss possible future developments. While a number of reviews of inelastic electron scattering [1–5] and inner-shell spectroscopy [6,7] have appeared over the years, there have been relatively few reviews focusing exclusively on ISEELS [8–12]. The excellent treatise on NEXAFS by Stöhr [7] includes a considerable number of dipole regime ISEELS spectra. A bibliography of inner-shell excitation spectral studies of gas phase atoms and molecules has been published [13] and updates are available on request from the author. In the context of this special issue on recent developments of instrumentation and applications of electron

spectroscopy, this review stresses mainly recent applications. However some key aspects of ISEELS instrumentation are described, with emphasis on aspects which lead to the special properties of ISEELS relative to X-ray absorption spectroscopy, and on aspects that will lead to improved future performance.

Although reports of X-ray absorption spectra of gases appeared sporadically as far back as 1934 [14], there was very little systematic investigation of core electronic excitation spectroscopy until several inelastic electron scattering instruments were developed. The first known report of ISEELS of a molecular gas was that by Van der Wiel, El-Sherbini and Brion [15] which showed the core electron excitation features of N_2 and CO recorded with a remarkable instrument constructed by Van der Wiel and collaborators at the FOM Institute for Atomic and Molecular Physics in Amsterdam. This instrument performed a wide range of energy loss and electron-ion coincidence studies, mainly in valence ionization [16] although with some core excitation contributions [17–21]. It provided the first absolute oscillator strength data from ISEELS [19]. The FOM spectrometer still operates today in Chris Brion's lab in the University of British Columbia (UBC) in Vancouver. Its outstanding success at simulating a number of UV and soft X-ray photoionization spectroscopies lead to the description of energy-loss based techniques which use high energy electron impact as the *poor man's synchrotron*. Several instruments working in the small scattering angle, high impact energy dipole regime were developed in the 1970s in UBC and used for systematic exploration of inner shell excitation spectroscopy of small molecules [22–34]. Prior to 1980 very few X-ray absorption studies of gases had been carried out largely because of the limited availability of synchrotron radiation and soft X-ray beam lines.

The first *high resolution* inner shell electron energy loss (ISEELS) studies were carried out in 1976 by Tronc, King and Read [35], soon followed by Hitchcock and Brion in 1977 [29]. The Manchester studies were initially in the dipole regime [35–44], but then, in the first exploitation of one of the unique aspects of ISEELS, they were extended to the non-dipole, near-threshold regime [45–47]. For over a decade, until the late-1980s, the energy resolution

of state-of-the-art ISEELS was generally superior to that of X-ray absorption spectroscopy. However, that situation changed rapidly with the development of high-performance spherical grating ('Dragon'-type) [48–51] and plane grating ('SX-700' type) monochromators [52–54] in the late 1980s and early 1990s. Currently, although competitive energy resolution is achieved with the highest performance ISEELS spectrometers, the field of high sensitivity, high energy resolution core excitation spectroscopy is dominated by synchrotron radiation.

Does this mean ISEELS is a dead technique? Not so. Today gas phase ISEELS is a powerful technique with many useful complementary aspects to synchrotron-based X-ray absorption spectroscopy of gases. ISEELS has remarkable advantages for: quantitative spectrometry; accuracy of energy scales; ability to study reactive systems; as well as unique capabilities for non-dipole spectroscopy and quantitative generalized oscillator strength profile measurements. Of particular note is the ability of ISEELS to provide absolute oscillator strengths in both dipole and non-dipole scattering conditions. This review stresses these aspects of ISEELS.

Of course experimental studies only provide the raw data for inner shell spectroscopy and spectrometry. Complementary theoretical studies are required to properly interpret results. This aspect has seen tremendous growth over the past 20 years, in part because of the vast improvements in computers and quantum computation codes. There is insufficient space to describe fully the theoretical work on core excitation that parallels development of experimental capabilities. In the area of dipole excitation the contributions of Peyerimhoff [55,56], Schwarz [6,57–59], Schirmer [60,61], Ågren [62–64] and Kosugi [65–67] are noteworthy for developing conceptual aspects. Recently quantum codes optimized to treat core electronic excitation have become more accessible and it is now practical for experimental groups to perform computations that help interpret their results. In my group, we first used the empirical extended Huckel method [68–70] and the equivalent ionic core virtual orbital model (EIC-VOM) [57,58] to treat inner shell excitation processes. Notwithstanding its quantitative limitations, this simple approach, which can be implemented very rapidly and effectively using the Computer

Aided Composition of Atomic Orbitals (CACAO) package [71], is remarkably powerful for developing a qualitative understanding of the links between core spectra and chemical trends. For the past five years we have been using Kosugi's *ab initio* Gaussian Self-Consistent Field 3 (GSCF3) code [65–67], which provides remarkably accurate core ionization potentials (IPs) and excitation energies for the lowest energy states. The improved virtual orbital (IVO) approximation often used with GSCF3 is conceptually similar to Agren's static exchange (STEX) method [62–64]. Recently Chong [72,73] has shown that density functional theory can provide very accurate core IPs and excitation energies. In the area of the theory of non-dipole core excitation by electron impact, there have been useful contributions by Schwarz [59] and by the Rio de Janeiro groups of Bielschowsky and Nasciemento [74–77].

2. Instrumentation and technique

2.1. Historical perspective

ISEELS began with Marnix Van der Wiel's 'poor man's synchrotron', a versatile, high impact energy, zero-scattering angle instrument which was developed around 1970 and used for simulations of dipole excitation (e,e') and ionic fragmentation (e,e',ion) of valence and inner-shell levels of molecules [15–21]. In 1973 Van der Wiel and Brion developed the corresponding dipole ($e,2e$) technique which simulates photoelectron spectroscopy, but that technique was only able to achieve inner-shell sensitivity in the hands of Thomas and coworkers who demonstrated the poor man's synchrotron equivalent to photon-excited auto-ionization spectroscopy [77–82]. Wight and Brion developed the second inner-shell electron energy loss system which was the first energy loss spectrometer dedicated to ISEELS studies. This unmonochromated, forward scattering instrument, rather similar in concept and capability to the current McMaster ISEELS spectrometer (Fig. 1), produced a remarkable series of publications [22–28] which, in a period of 2 years, increased the size of the inner shell electronic excitation data bank more than ten-fold. Throughout the 1970s and 1980s, the Brion group continued to

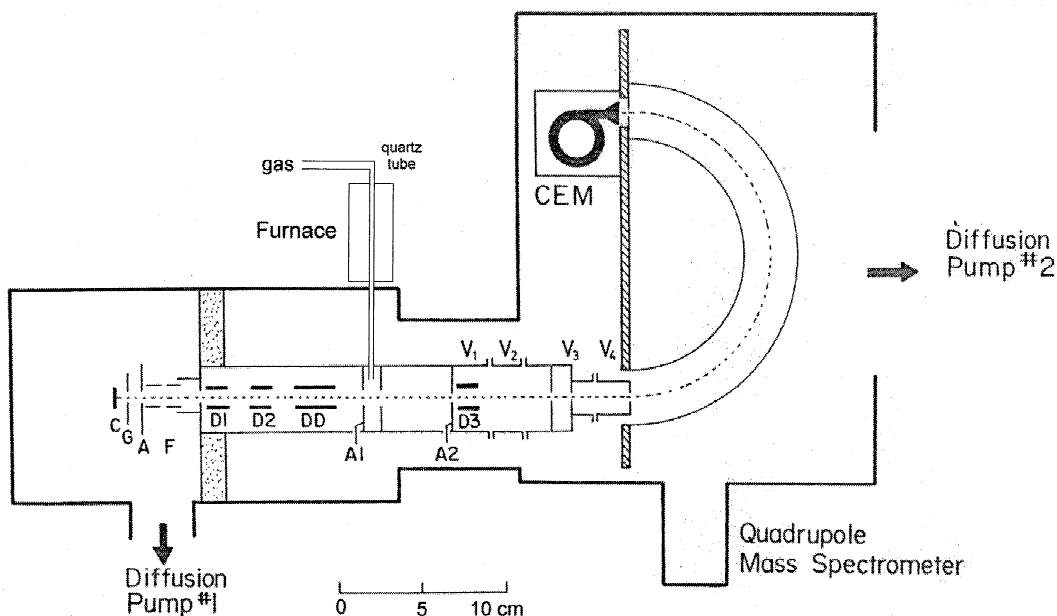


Fig. 1. Schematic of the unmonochromated inner shell electron energy loss spectrometer (ISEELS) at McMaster [9–12]. The instrument is operated in constant final energy mode, typically with a final energy of 2.5 keV. The scattering angle can be adjusted in the $\pm 6^\circ$ range by electrostatic deflection. The sample introduction system illustrated, one of a number, is that used recently for transient studies [125].

advance the field, developing a first-generation monochromated forward scattering instrument and then a second generation, high performance, fully optimized monochromated forward scattering spectrometer, ‘Superspec’ [83] (Fig. 2).

The Manchester spectrometer developed by Read and King, which produced the first high resolution dipole regime monochromated ISEELS spectra [35], was a zero degree instrument capable of operating at a range of impact energies. The first ISEELS spectrometer at Manchester established a level of performance that has only been equaled, but not surpassed with later spectrometers. The variable impact energy capability of the Manchester instrument was also used to record non-dipole ISEELS spectra at high resolution [42–45], including the first detection of the vibrational structure of non-dipole inner-shell excited states of molecules [45].

In the mid-1980s, the first McMaster instrument was developed and used for systematic investigations of chemical series [10,11]. At the same time, King and Harrison developed an unmonochromated, 90° scattering angle spectrometer in Manchester and carried out the first systematic studies of non-dipole

ISEELS, using a fixed, large scattering angle (90°) and near threshold impact energies [84–86]. The McMaster variable angle, high resolution energy spectrometer (McVAHRES, Fig. 3) was developed between 1992 and 1995. It was designed to cover the full range of electron impact scattering conditions, from near threshold to high impact energy, with scattering angles from -10° to $+110^\circ$ [87,88]. A number of high resolution studies have been performed with McVAHRES [89–91] but more recently it has been dedicated to measurements of the impact energy and scattering angle dependence of inner shell excitation intensities which are typically condensed to generalized oscillator strength (GOS) profiles [92–96]. Prior to that work, relatively few detailed studies of the GOS of specific core states had been carried out. Early studies by Bonham and Wellenstein gave overviews of the Bethe surfaces of some molecules [3,5,97–100] but little or no detail as to the GOS profiles of individual core excited states.

In the 1980s and 1990s other research groups also started ISEELS programs, often as a complement to other uses of the same instrument. Thus Stefani and

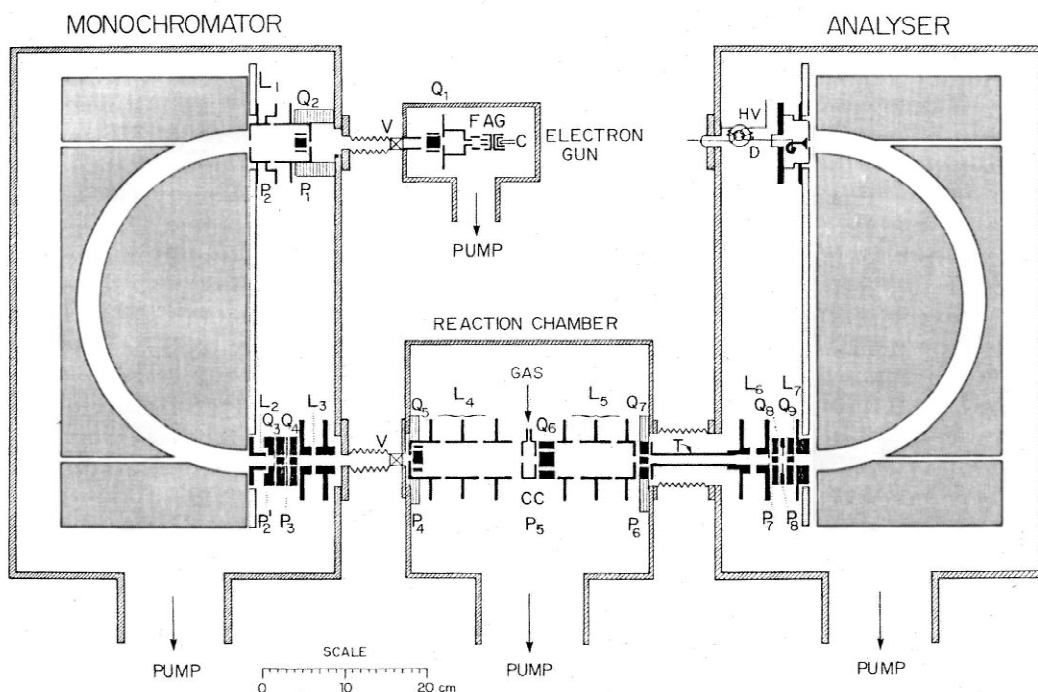


Fig. 2. Schematic of the multi-chamber, monochromated electron energy loss spectrometer at the University of British Columbia ('superspec') which is used for both valence and inner shell excitation studies. The impact energy is typically 3.5 keV. The scattering angle can be adjusted in the $\pm 3^\circ$ range by electrostatic deflection [83].

coworkers adapted a binary ($e,2e$) variable scattering angle system for some non-dipole ISEELS, including mapping of the GOS profile of the strong $1s \rightarrow \pi^*$ transition of N_2 in a coordinated experimental — theoretical effort to detect signal from the dipole forbidden ($N 1s \sigma_u^{-1}, \pi_u^*$) $^1\Pi_g$ state [101–103], and to derive the GOS profile for the Rydberg states of Ne [104]. Similarly Leung et al., adapted the Waterloo binary ($e,2e$) spectrometer to measure valence and inner shell GOS [105,106]. DeSouza (Rio de Janeiro) [107,108] and Moore (Maryland) [109–111] are performing ISEELS on spectrometers originally constructed for variable angle valence EELS. Hubin-Franskin (Liege) adapted a surface analysis instrument to become the first ISEELS system with a CCD-based parallel detector [112] and has used it for a number of elegant gas phase inner-shell studies [113–115]. At present the only energy loss spectrometers completely dedicated to gas phase ISEELS studies that are in regular operation are the two instruments at McMaster (Hamilton) and Superspec

at UBC (Vancouver). In addition there are shared-use systems operating in Vancouver, Rome, Rio de Janeiro, Maryland, and Waterloo. Table 1 summarizes all instruments — past and present — which have been used for ISEELS studies to my knowledge.

2.2. Instrumentation aspects — current themes

While electron impact spectrometers can be constructed with lenses and analysers based on electrostatic fields, magnetic fields, or a combination of both, most systems use fully electrostatic technologies since these are easier to implement. Reviews of electron scattering which stress instrumentation have been published by Bonham [2,4], Lassetre [3] and Kerwin et al. [116], while other reviews of electron spectroscopy contain significant components on instrumentation [117]. The reference book on electrostatic lenses by Harting and Read [118] is a bible for electron spectrometer design.

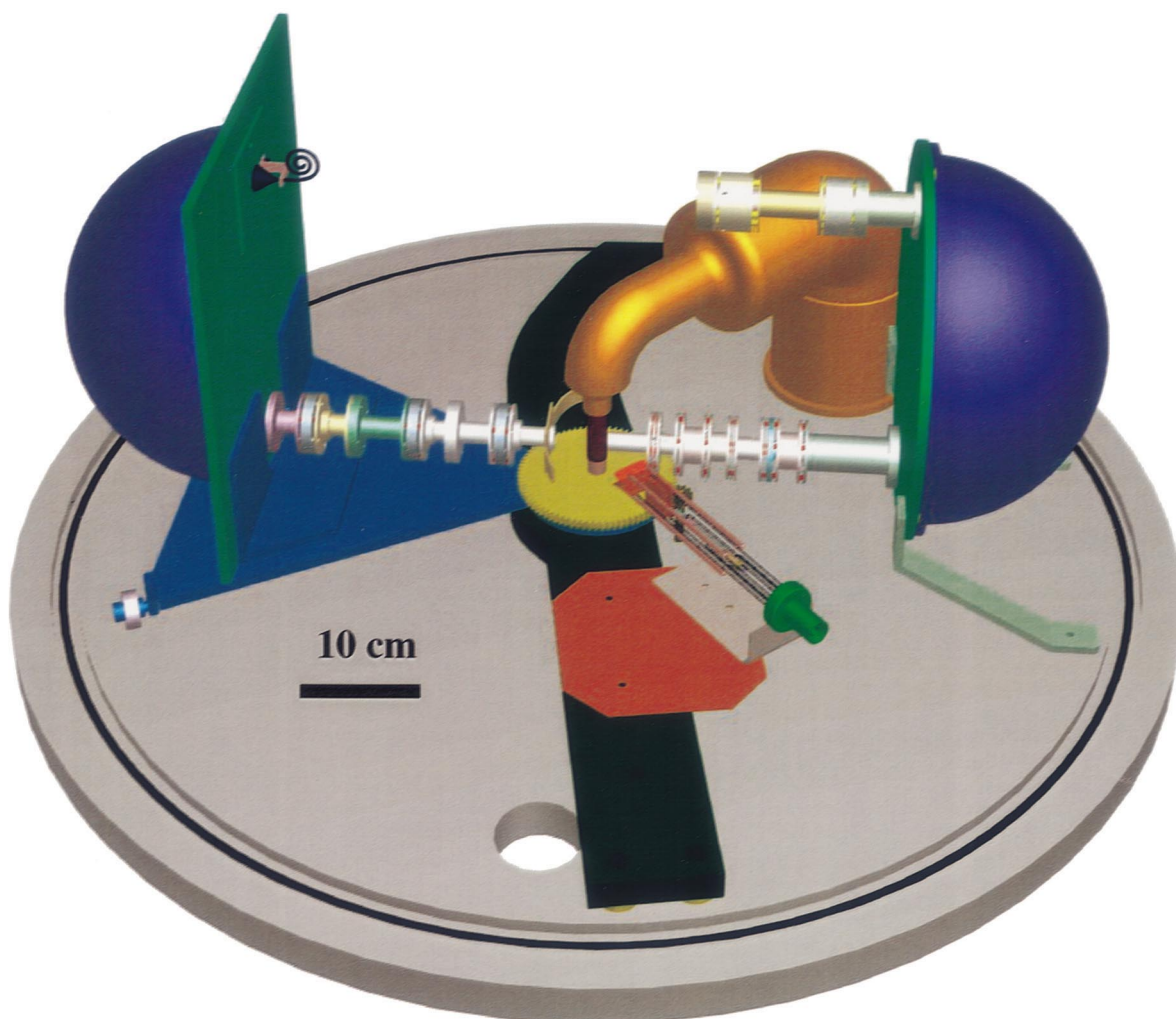


Fig. 3. The McMaster Variable, Angle High Resolution Electron Spectrometer (McVAHRES) [88]. The analyzer is shown positioned at zero degree scattering angle relative to the monochromated electron beam and at 60° scattering angle relative to the un-monochromated electron beam. Scattering angles can be varied from -10° to $+110^\circ$ (unmonochromated) or -35° to $+85^\circ$ (monochromated). The instrument can be operated with final electron energies from 100 to 2000 eV. The sample at the center of the chamber is either an effusive gas jet or an enclosed collision cell. A pumping port positioned directly over the jet provides a tenfold differential pressure between the sample region and the remainder of the spectrometer. The spectrometer is shown with a single channel, channeltron detector. Recently a high efficiency position sensitive, 2-d resistive anode parallel detector [124] has been installed.

Recently electron lens design computer software based on the Harting and Read data base adapted to take into account space charge effects has become available [119]. Descriptions of the electron optics of individual spectrometers [83,113–115,120] also provide useful information on design and construction principles. The principles of optimization of lenses analysers and mechanical aspects have changed little

for many years [121–123]. Recent trends in EELS instrumentation include extensive use of computer-controlled power supplies and motors; fully integrated control, acquisition and presentation software; and use of one-dimensional and two-dimensional parallel detection [112]. The latter development is common in synchrotron based photoelectron spectrometers, and a few lab-based energy loss systems,

Table 1
Summary of inner shell electron energy loss spectrometers

Date	Group	Location	E_0 (eV)	θ°	Comments
1969–76	Van der Wiel	Amsterdam	3500	0	(e,e') (e;e,ion)
1976–now	Brion	Vancouver	3500	0	(e,e') (e;e,ion)
1972–76	Brion	Vancouver	2500	2	
1975–92	Brion	Vancouver	2500	2–6	Monochromated (Vincent)
1975–95	Bonham	Indiana	25 keV	1–130	GOS
1976–84	Read	Manchester	50–2000	0	Monochromated
1976–now	Bennani	Paris	25 keV	0–45	(e,2e)
1984–now	Wellenstein	Waltham	25 keV	1–130	(e,e'), GOS
1984–90	King	Manchester	200–1000	90	Threshold
1980–now	Brion	Vancouver	1.5– 5 keV	0	Monochromated
1980–now	Hitchcock	Hamilton	2500 + loss	2–6	(ISEELS)
1982–96	Thomas	Corvallis	3000	0.54	(e,2e)
1985–now	Stefani	Rome	2000	–20–90	(e,2e)-adapted, GOS, EXELFS
1985–now	Moore	Maryland	2000	10–60	Shared use
1990–now	de Souza	Rio de Janeiro	1500	2–30	Shared use
1994–now	Hubin-Franskin	Liege	2000	1	Shared use
1992–now	Leung	Waterloo	2500	10–30	GOS
1994–now	Hitchcock	Hamilton	50–2000	–10–110	Mono; GOS (McVAHRES)

but it is not yet common in ISEELS. However parallel detection will enable tremendous advances in ISEELS since the cross sections for core excitation are very weak, particularly in the non-dipole and threshold regimes. Recently a 2-d resistive anode position sensitive detection system [124] has been installed on the McMaster variable angle high resolution electron spectrometer (McVAHRES) which has provided a ~ 40 -fold improvement in signal rates.

The first McMaster ISEELS spectrometer [9–12], depicted schematically in Fig. 1, is typical of unmonochromated instruments. The electron source is a black and white television tube electron gun, which produces a high intensity, parallel, small beam. Right after activation the oxide cathode gun provides a 0.3 mm diameter beam with up to 40 μA current at 2.5 keV. At 4 μA current the energy spread is less than 0.4 eV, but rises to ~ 0.7 eV with currents above 20 μA due to space charge effects. Another important advantage is that these guns are very inexpensive and thus it is practical to use them as a disposable item in studies of chemically reactive molecules, which often destroy the sensitive barium strontium oxide emitting surface in a few hours or days.

The electron scattering column consists of a number of quadrupole deflection plates, apertures and a four-element deceleration lens, all made from brass, except for the aperture plates which are made

from molybdenum, in order to withstand the heat load. There is no provision for changing scattering geometry mechanically, and thus the scattering angles are restricted to $\pm 6^\circ$ which is achieved with electrostatic deflection. An important practical aspect of this spectrometer is the double deflection system which allows the main beam to traverse the high gas density in the center of the collision cell, but be intercepted at aperture plate, A2. This is critical since very large backgrounds occur when the main beam enters the analyzer, due to scattering from the outer hemispherical surfaces. The double deflection system ensures the incident electron beam, high gas density and analyzer acceptance cone have maximum overlap in the same volume. The typical scattering angle is 2° with an integrated acceptance of $\sim 1^\circ$. The analyzer, a set of graphite-coated, machined stainless steel hemispheres, is typically operated at 40 eV pass energy, for an overall incident beam and analyzer resolution of 0.5–0.7 eV, depending on the incident beam current. Those inelastic scattered electrons which, after deceleration, have the analyzer pass energy, go through the 1-mm exit aperture, and are detected by a channeltron. In addition to the energy loss signal, the acquisition system records gas pressure and incident beam current, which can be used for point-by-point normalization.

The unmonochromated McMaster spectrometer

has a number of different ways of introducing samples, including a conventional leak valve line for permanent gases and high vapor pressure liquids, and a solids probe system. The latter system, when used in combination with an internal quartz bulb heater embedded in the wall of the collision cell, and water-cooled plates above and below the collision cell, allows measurements of solids which have very low vapor pressure, including species with melting points above 300°C. The ISEELS instrument was adapted recently for transient studies by coupling a thermal reactor to the solids probe inlet as depicted in Fig. 1. With this system, the collision region can be heated to about 200°C and the vapor products from thermal reactions up to 1200°C can be studied [125] (see below).

The second system illustrative of modern ISEELS is the ‘Superspec’ spectrometer in Brion’s laboratory at UBC (Fig. 2) [83]. This instrument has produced among the highest energy resolution core excitation spectra as well as a large amount of high accuracy valence and inner shell dipole oscillator strengths [126,127], including absolute results for vibrationally resolved core excitation [128]. It is a large instrument — the monochromator and analyzer hemispherical sections are 60 cm tall, and the electron beam trajectory is more than 1 meter — with a fixed zero degree scattering angle geometry and 3.5 keV impact energy. The gun, monochromator, collision region, and analyzer are all in separately pumped vacuum chambers. The design principles for the electron optics, and an evaluation of its performance has been described in detail elsewhere [83].

The third system, arguably the most sophisticated of current ISEELS spectrometers in terms of the instrumentation principles and the range of experimental conditions under which it is capable of operating, is the McMaster Variable, Angle High Resolution Electron Spectrometer (McVAHRES) (Fig. 3) [88]. The design goal was to achieve a very flexible instrument for dipole, non-dipole and near-threshold core excitation studies. For this we have developed an instrument with two electron beam sources — an unmonochromated beam for high-efficiency studies of weak, large scattering angle signals, and a monochromated beam for high energy resolution studies. The instrument is operated in constant final electron energy mode [1], with the

residual energy variable from 50 to 2000 eV. Scattering angles can be varied from -10° to $+110^\circ$ (unmonochromated) or -35° to $+85^\circ$ (monochromated) with an angular resolution of 1° . The sample is either an effusive gas jet or an enclosed collision cell, at the center of the chamber. There is a pumping port positioned directly over the jet which provides about a ten-fold differential between the pressure in the sample region and the remainder of the spectrometer. Fig. 3 shows the spectrometer equipped with a single channel, channeltron detector with which most work to date has been carried out. Recently a high efficiency position sensitive, 2-d resistive anode parallel detector [124] has been installed. The first results recorded with this new detector are reported below.

One advantage of ISEELS over soft X-ray absorption spectroscopy is the ease with which very high accuracy transition energies can be measured. This is because it is easy to measure voltages accurately and thus the transition energy in ISEELS is readily referenced via a voltage scale to the elastic peak, or to a low energy valence excitation signal for which very accurate transition energies are known from optical studies. In fact the most accurate high resolution soft X-ray spectral energy scales are based on calibration to values provided by ISEELS studies [129,130] carried out to provide secondary reference standards for use in the soft X-ray spectral region.

Another aspect for which ISEELS has a significant advantage over soft X-ray absorption spectroscopy is the relative ease with which quantitative intensity scales can be established. First, because EELS is a non-resonant technique it does not suffer from absorption saturation problems which have been the source of many incorrect intensity scales in optical techniques [126,127]. Second, sum rule techniques [5,16,126,127] or normalization to tabulated atomic oscillator strengths [131] outside of the structured near edge region can be used to convert relative dipole regime ISEELS intensity scales to absolute photoabsorption oscillator strength scales [13,16,126–130]. Indeed, as long as the Born approximation holds, it is possible to use Bethe sum rules to place non-dipole ISEELS on an absolute scale. This is in strong contrast to optical spectroscopy where absolute scales are notoriously difficult to obtain.

2.3. High resolution performance

Fig. 4 presents variable impact energy ISEELS of CO in the region of the $(C\ 1s^{-1}, \pi^*)\ ^3\Pi$ and $(C\ 1s^{-1}, \pi^*)\ ^1\Pi$ states [90]. Fig. 4a illustrates vibrationally resolved core excitation as well as the ability to vary selection rules by changing scattering conditions. Fig. 4b is a detailed comparison of the vibrational band structure of the dipole $X\ ^1\Sigma^+ \rightarrow (C\ 1s^{-1}, \pi^*)\ ^3\Pi$ of CO and non-dipole $X\ ^1\Sigma^+ \rightarrow (C\ 1s^{-1}, \pi^*)\ ^1\Pi$ transitions. The peaks have been placed on common relative energy and intensity scales to facilitate line-shape comparison. This clearly shows that the Franck–Condon factors for the two states are different indicating that differences in the core-valence exchange interactions in these two states lead to significant changes in the potential energy surfaces. In conjunction with high level ab initio calculations, these results were able to quantify the differences in the potential curves for these two,

closely related states [90]. To my knowledge, the only other example of vibrationally resolved *non-dipole* ISEELS is the work of King et al. [45–47]. A much larger number of vibrationally resolved dipole ISEELS have been reported, not surprisingly given the much stronger cross-section in the dipole regime.

3. Results — recent applications

3.1. Linking ISEELS and electronic structure: chemical series

A common theme of many ISEELS studies (as in other electronic spectroscopies) is the examination of series of related molecules in order to better understand the dependence of the observed spectral structure on the molecular structure. Such studies improve our understanding of chemical bonding and assist in making predictions of the core spectra of molecules

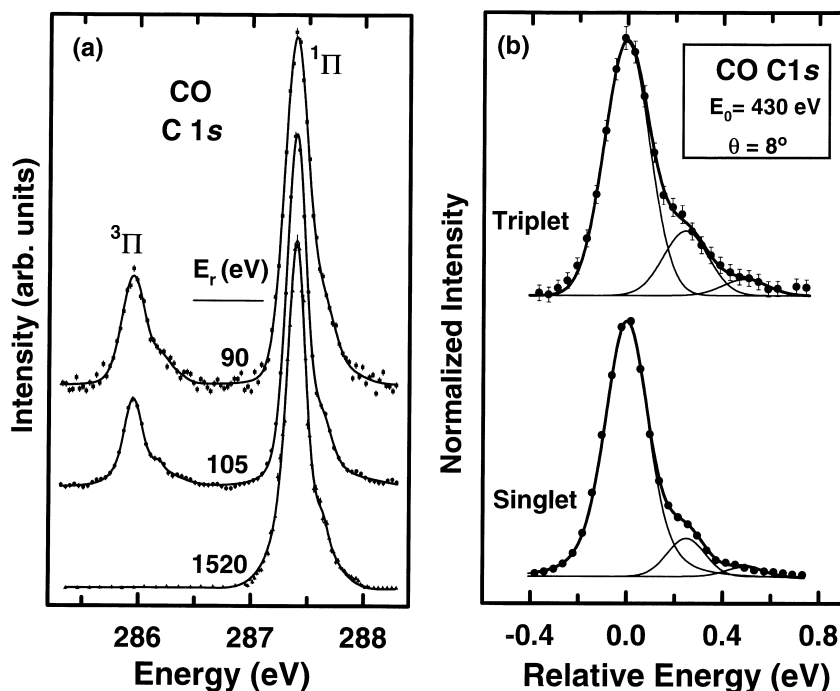


Fig. 4. (a) Impact energy dependence of the electron energy loss spectrum of CO in the region of the $(C\ 1s^{-1}, \pi^*)\ ^3\Pi$ and $^1\Pi$ states recorded with McVAHRES in monochromated mode at residual energies of 90, 105 and 1520 eV and scattering angles of 4° , 4° and 2° , respectively. (b) Comparison of the vibrational band structure of the $X\ ^1\Sigma^+ \rightarrow (C\ 1s^{-1}, \pi^*)\ ^3\Pi$ and $X\ ^1\Sigma^+ \rightarrow (C\ 1s^{-1}, \pi^*)\ ^1\Pi$ transitions. The peaks have been placed on a common relative energy scale and scaled to the same intensity of the $v=0$ peak to facilitate line-shape comparison. The triplet state spectrum was recorded at 140 eV residual energy, 8° scattering angle and 0.18 eV FWHM resolution [90].

or molecular fragments (e.g. repeat units of polymers) for which it is difficult or impossible to record reference spectra. A recent study of the inner-shell spectroscopy of nitroanilines [132] exemplifies this aspect of ISEELS. The *ortho*, *meta* and *para* nitroaniline isomers are of interest since there is strong interaction of the donor (NH_2) and acceptor (NO_2) substituents in these ‘push–pull’ molecules which has been speculated to have dramatic effects on various spectroscopies, including predictions of a surprising ‘shake-down’ feature in the N 1s X-ray photoelectron spectrum [133]. If these two substituents contributed in a relatively independent way

to the total C 1s, N 1s and O 1s core excitation spectra one might expect the inner shell spectra of the three isomers to be similar to each other. Further, the so-called ‘building block’ picture of core excitation [7] predicts the nitroaniline spectra should be similar to an appropriately weighted sum of the spectra of nitrobenzene and aniline. One goal of the study [132] was to test these hypotheses. They turn out to be reasonable for the O 1s spectra but we found significant deviations in the C 1s and N 1s spectra. Fig. 5a compares the C 1s ISEELS spectra of *ortho*-, *meta*- and *para*-nitroaniline with a simulation generated by a weighted sum of the C 1s

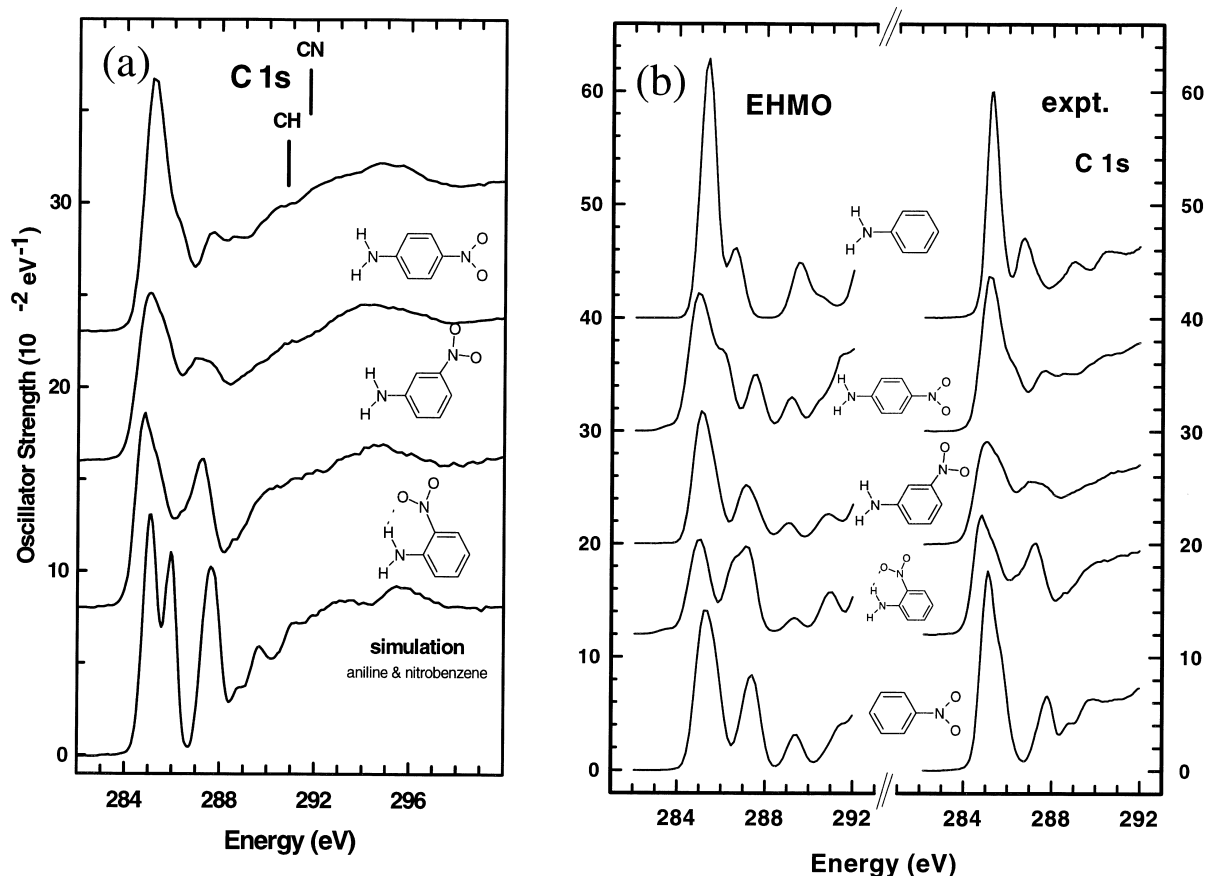


Fig. 5. (a) The C 1s dipole regime ISEELS spectra of *ortho*-, *meta*- and *para*-nitroaniline compared to that of a simulation generated by the sum of the C 1s ISEELS spectrum of nitrobenzene (shifted by -0.1 eV) and aniline (shifted by $+0.5$ eV). The shifts correct for electrostatic shifts in forming the di-substituted benzene and are taken from XPS. (b) EHMO — EICVOM computed C 1s spectral shapes compared to experimental spectral shapes for aniline, *ortho*-, *meta*- and *para*-nitroaniline and nitrobenzene. The energy scales for the spectra derived from the EHMO calculations have been adjusted to align the first π^* feature with experiment. Relative to alignment at the experimental IPs, this required shifts of 4.4, 3.5, 3.2, 3.3 and 3.2 eV respectively (averages over all C sites) [132].

ISEELS spectra of nitrobenzene (shifted by -0.1 eV) and aniline (shifted by $+0.5$ eV). These shifts correct for electrostatic shifts in forming the di-substituted benzene and are taken from XPS [132]. It is very clear that the simulated and measured isomeric spectra differ significantly in the region of the discrete structure, indicating there are geometry specific aspects of the interaction of the two substituents. The nature of these interactions has been explored using extended Huckel molecular orbital calculations within the equivalent ionic core virtual orbital model (EICVOM) [57,58]. Fig. 5b compares the EHMO-computed spectral shapes to the experimental spectral shapes for the discrete region of the C 1s spectra of aniline, *ortho*-, *meta* and *para*-nitroaniline and nitrobenzene. While all features are not reproduced, the main aspects of the spectral dependence are tracked by these calculations, which include contributions from excitation at each chemically distinct carbon in each molecule [132]. The distinction between *ortho*-, *para*-directing and *meta*-directing aspects of π -interacting substituents, as well as H-bonding in *ortho*-nitroaniline help explain how the C 1s spectra depend on the pattern of substitution. For many more details on the spectroscopy, the calculations and the conceptual interpretation the interested reader is referred to [132]. A dependence of the fine details of C 1s spectra on isomeric substitution patterns has been documented in a number of other systems, including dimethylphthalates [134], and xylenes [135]. While there are some common aspects, because there are a number of factors involved it is important to evaluate on a case-by-case basis when considering the potential of core excitation spectroscopy as an analytical tool for determining substitution patterns in di-substituted aromatic rings.

A second example of a chemical series study is one taken from a larger body of work in which ISEELS spectra of gases [134,136–142] are being used to help interpret NEXAFS and X-ray spectromicroscopy spectra of polymers [143]. Fig. 6 compares the C 1s dipole regime ISEELS spectra of ethylbenzoate and 1,4-dimethylphthalate (1,4-DMP) with the photoabsorption spectrum of polyethyleneterephthalate (PET) [134,139,141]. Here we are using molecular analogues to model the core spectrum of a polymer. Even though the local

bonding in ethylbenzoate, 1,4-DMP and PET are virtually identical, the C 1s spectrum of PET differs from that for 1,4-DMP, and especially from that of ethylbenzoate, beyond the trivial differences arising from the fact that the resolution of the X-ray spectrum (~ 0.3 eV fwhm) is higher than that of the ISEELS (0.6 eV fwhm). This indicates that longer range through-bond and through-space interactions among adjacent repeat units does influence core excitation spectra, and thus there can be significant errors in the simple building block [7], additive approach to core spectra. The breakdown of the building block model is dramatically illustrated in Fig. 6 by comparison of the spectrum of ethylbenzoate (already not a bad model for PET [139,141]) with a simulation consisting of a weighted sum of the C 1s spectra of benzene [144] and formic acid [145]. The ~ 0.3 eV decrease in the position of the main C 1s(C–H) $\rightarrow\pi^*_{C=C}$ transition and the appearance of two additional $\pi^*_{C=O}$ structures around 290 eV are related to delocalization interactions in the π^* manifold [7]. While the breakdown of a simple additive model can be considered a limitation, in fact, the additional sensitivity to longer range interactions provides a tool that could be extremely useful analytically. For example differences between the core excitation spectra of gas [146] and solid [147] carboxylic acids are believed to arise from hydrogen bonding which only exists in the solid state. The rapid increase in use of NEXAFS spectroscopy and microscopy [143] for investigations of polymers will lead to a better understanding of the extent to which core spectra are influenced by intermolecular interactions such as hydrogen bonding since these are an important theme in explaining polymer bonding and properties.

3.2. ISEELS spectroscopy of transient species

A popular application of valence shell photoelectron spectroscopy (PES) is in situ analysis of chemical reactions [148,149] — transient photoelectron spectroscopy. In many cases, information about the electronic structure of reaction intermediates and reactive products helps to understand reaction mechanisms. Gas phase inner shell spectroscopy studies of reactions can provide useful complementary information, with potential for superior performance in

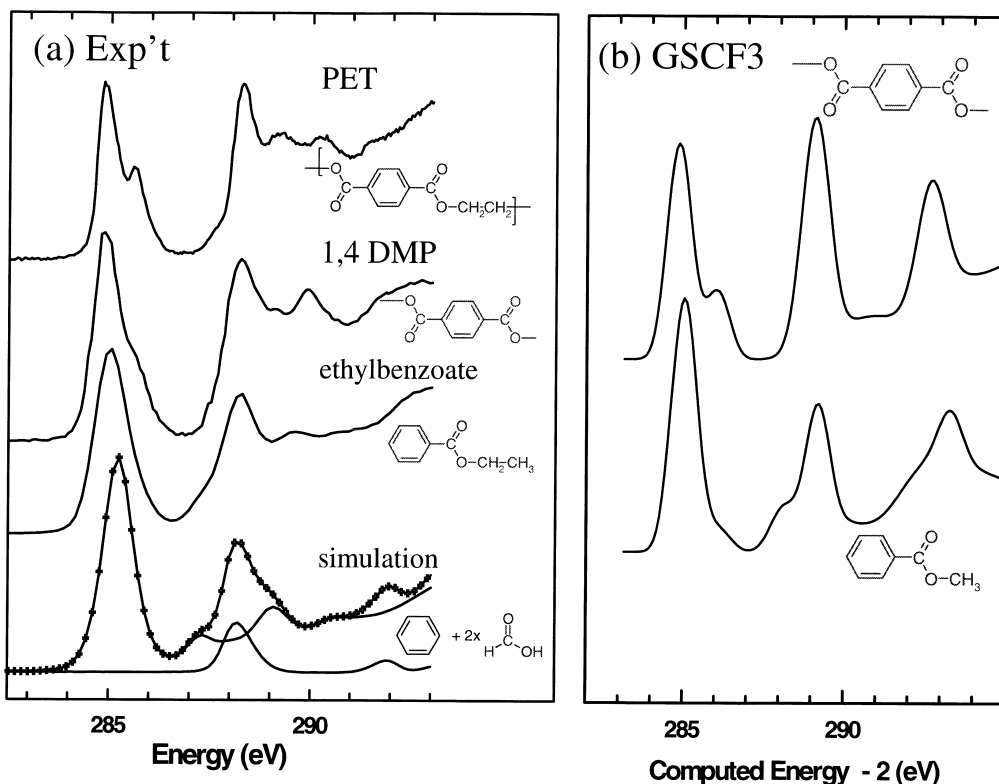


Fig. 6. (a) Dipole regime C 1s ISEELS spectra (2.5 keV final energy, $\theta=2^\circ$) of ethylbenzoate and 1,4-dimethylphthalate compared to the synchrotron X-ray photoabsorption spectrum of polyethyleneterephthalate [142,143], and a simulation consisting of a weighted sum of the C 1s spectra of benzene [144] and formic acid [45]. The changes with molecular structure in the core excitation fine structure, which are closely related to delocalization interactions in the π^* manifold, are an important caution about the limitations of the building block model [7]. (b) GSCF3-calculated C 1s spectra of 1,4-dimethylterephthalate and methylbenzoate. Note the 2-eV shift in the presentation relative to the computed energy scale (Urquhart, private communication).

some aspects. The ability to look at a number of different core edges quasi-simultaneously provides elemental analysis. When combined with in situ mass spectrometry, this can be very helpful when studying a poorly characterized reaction. ISEELS has better sensitivity to low yield processes than PES since the gas density required is several orders of magnitude lower. Finally, but perhaps most important, the insight into bonding and electronic structure provided by core excitation, a site- and symmetry-specific probe of unoccupied electronic structure, is highly complementary to that of PES, which probes the occupied valence levels.

In principle synchrotron X-ray absorption could be a tremendous tool for transient studies. However, procedures required to mount a potentially dangerous

chemical reaction at a synchrotron facility are usually so strict as to present a significant activation barrier to this type of project. In contrast lab-based ISEELS in an environment properly equipped for reaction chemistry is a more straightforward proposition. We have recently started a program to develop methods and applications of transient-ISEELS. Our first work was an exploration of reactions involving divalent, di-coordinate silicon, an unusual oxidation state that has recently been isolatable in compounds stabilized by ring delocalization and bulky substituents [150,151]. These stable but highly reactive compounds have tremendous potential as synthetic agents [152]. Spectroscopic probes of their reactions can help develop this potential by aiding a proper understanding of the reaction mechanisms. Two

transient reactions in this area were explored with ISEELS in 1997 and 1998 [153]. A full explanation of these complex observations is still under development. In 1998–99 we decided to demonstrate the validity of transient-ISEELS by studying a reaction system previously studied by transient-PES, the formation of HBS from the heterogeneous reaction of hydrogen sulfide and boron [154,155]. The ISEELS results fully reproduced the chemistry tracked by transient-PES. In addition, to our surprise and satisfaction, we were also able to identify a new product in the reaction [125], one which has never been studied with photoelectron spectroscopy, although it had been identified as a trace component by mass spectrometry and investigated with other transient spectroscopies. As with series of stable chemical compounds, we have used quantum chemistry, in this case *ab initio* GSCF3 calculations, to support our interpretation of the transient chemistry, to assign the ISEELS spectra, and to better understand the spectral–structure relationships.

Fig. 7 presents dipole-regime ISEELS spectra (2.5 keV final energy, $\theta=2^\circ$) recorded on the gas phase output (10^{-5} Torr) of a heated quartz tube through which H_2S is passed over boron crystals [125]. The relationship of the furnace and the spectrometer is indicated in Fig. 1. At furnace temperatures above 1050°C the H_2S signal disappears and converts to S 2p, S 2s and B 1s signals consistent with complete conversion to HBS. Further heating to 1200 – 1250°C results in almost complete loss of S 2p signal, and a modified B 1s spectrum which is interpreted as that of HBO. Quadrupole mass spectrometry of the vapor in the spectrometer fully support our interpretation of the transient chemistry [125] although the ISEELS spectrum was actually a much more sensitive probe since the vapor molecules suffer several potentially reactive wall collisions before entering the mass spectrometer, which is distant from the collision region (see Fig. 1). Detailed comparison was made of the S 2p, S 2s, B 1s and O 1s inner shell spectra among the stable and transient species, and with simulated spectra based on GSCF3 *ab initio* calculations. The B 1s spectra (inset to Fig. 7) showed that the spectrum produced under the most extreme furnace conditions which is attributed to that HBO is distinct from the B 1s spectrum of the more stable $\text{H}_3\text{B}_3\text{O}_3$ trimer which is produced when water is

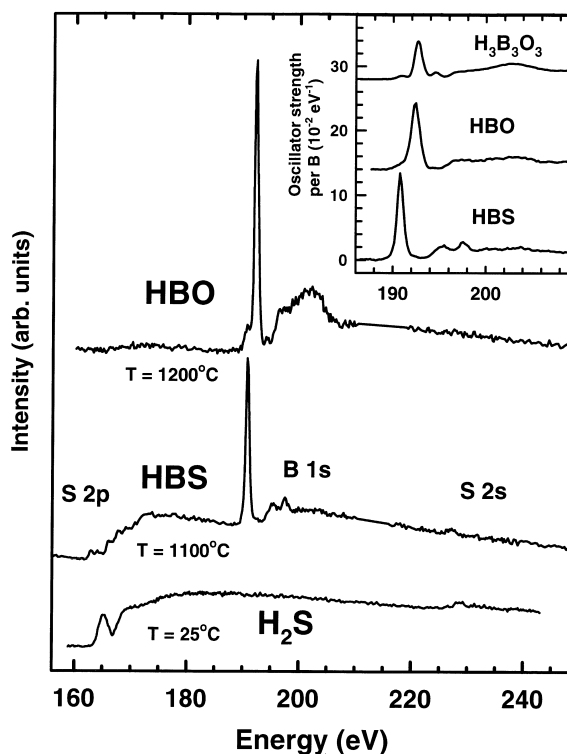


Fig. 7. Dipole-regime ISEELS spectra (2.5 keV final energy, $\theta=20^\circ$) of the output of a heated quartz tube through which H_2S is passed over boron crystals [125]. At furnace temperatures above 1050°C the H_2S signal disappears and converts to S 2p, S 2s and B 1s signals which are consistent with complete conversion to HBS. Further heating to 1200 – 1250°C results in almost complete loss of S 2p signal, and a modified B 1s spectrum which is interpreted as that of HBO. The inset compares the B 1s spectra from the two regimes of the ($\text{H}_2\text{S}/\text{B}(\text{s})/\text{quartz}$) high temperature reaction with that from the corresponding $\text{H}_2\text{O}/\text{B}(\text{s})$ reaction, which is known to produce the thermodynamically preferred $\text{H}_3\text{B}_3\text{O}_3$ trimer [125].

passed over hot boron [154]. Our studies suggest that attack of quartz by H_2S at high temperature can be a useful means to produce small amounts of reactive oxygen. This could be developed as a means for controlled partial oxidation for use in transient studies or even synthetic applications [125].

3.3. Non-dipole spectroscopy

One of the major advantages of electron energy loss spectroscopy over photoabsorption spectroscopy is the ability to probe excited states which are not

electric dipole coupled to the ground state. This allows ISEELS to provide a more complete investigation of the inner shell excited states of the target. When the incident electron is highly energetic (large E_0) and is scattered through a small angle, the momentum transferred to the target from the colliding electron is very small, the interaction between this electron and the target is weak, and electric dipole processes dominate. Most of the results described so far were recorded in that so-called dipole-regime and thus can be interpreted in the same framework as the corresponding X-ray absorption spectra. However, when the scattering angle becomes large ($>10^\circ$), the momentum transferred to the target from the incident electron during the collision increases. This results in relaxation of the electric-dipole selection rules, typically resulting in excitation of higher order electric multipole transitions [2,156]. One way to determine if a given transition is dipole allowed (perhaps via a vibronic mechanism) from one which is dipole forbidden, is to see if the relative intensity of that feature increases relative to the intensity of known dipole features as the scattering angle increases. Another non-dipole ISEELS regime is near-threshold. When the impact energy is reduced to only slightly higher than the transition energy, spin forbidden electronic transitions can be excited with significant probability on account of the exchange interaction of the incident and target electrons. We have used all of these modes in systematic studies of non-dipole inner-shell spectroscopy of gases [87–96]. The data on CO [90] presented in Fig. 4 exemplifies the threshold situation. The work by the Manchester group [45–47,84–86] is the most significant and comprehensive contribution in the area of threshold ISEELS.

As an illustration of novel non-dipole ISEELS spectroscopy, Fig. 8 compares dipole regime (1.5 keV final energy, $\theta=4^\circ$) and non-dipole regime (1.5 keV final energy, $\theta=62^\circ$) spectra of SF_6 [95] recorded with the McVAHRES instrument [88]. The peak at 183 eV, labelled B, had not been identified in the literature prior to our first systematic study of the non-dipole spectroscopy of SF_6 [91], yet it becomes the most intense S 2p spectral feature at scattering angles above 40° , when the impact energy is large. Interestingly it is relatively weak again under near-threshold conditions where the momentum transfer is

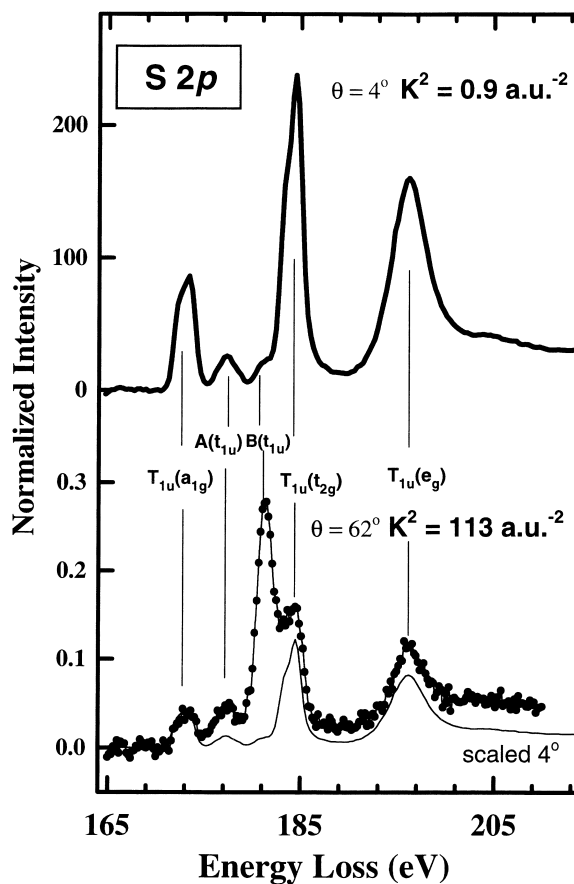


Fig. 8. Comparison of dipole regime (1.5 keV final energy, $\theta=4^\circ$) and non-dipole regime (1.5 keV final energy, $\theta=62^\circ$) spectra of SF_6 [95] recorded with McVAHRES [88]. The peak at 183 eV, labelled B, was not noted in the literature prior to our earlier non-dipole study [91], yet it becomes the most intense S 2p spectral feature at scattering angles above 40° , when the impact energy is large.

low [95]. A similar large change is seen between dipole and non-dipole S 2s spectra [95] whereas the shape of the F 1s spectrum of SF_6 is essentially independent of momentum transfer [88], even though non-dipole F 1s excitations do exist. Understanding these unusual dependencies of relative spectral intensities on scattering conditions is a goal of our systematic angle- and impact energy studies. Since our results for core excited states of molecules extend to the dipole regime we choose to report them as apparent generalized oscillator strength profiles even though at high momentum transfer there is a

possibility of breakdown of the first Born approximation such that the GOS concept is no longer valid [156].

3.4. Non-dipole spectrometry: generalized oscillator strength profiles

Since 1994 McVAHRES has been used for systematic measurements of the angular dependence of ISEELS intensities in order to investigate the relationship between inner shell GOS profiles and molecular electronic structure. While this type of information was generated for many valence electronic excitations of molecules in the 1960s and 1970s, primarily by Lassetre and co-workers [2], this is the first systematic approach to studying the corresponding signals for inner shell electronic excitation. Some of the questions which motivate this work include:

- What types of molecules/electronic structure motifs lead to structured GOS profiles? Can the shapes of angular profiles be used as a diagnostic for aspects of the transitions and/or states involved, such as symmetry or Rydberg/valence character of the upper level?
- Do angular profiles provide a means of discovering new electronic states?
- Can GOS profiles provide information about important themes of core excitation spectroscopy such as core hole localization and shape resonance dynamics?

We have chosen to express the angular intensities on a uniform quantitative generalized oscillator strength scale [156], in order to reduce the dimensionality of the problem relative to a differential cross section representation [2], and thus to facilitate comparison between theory and experimental results obtained with a variety of electron impact energies. The GOS concept is strictly correct only under conditions where the first Born approximation (FBA) holds, which can be defined experimentally as that regime in which the apparent GOS at a given momentum transfer is constant over a range of impact energies [156]. Valence EELS studies suggest the FBA breaks down as low as 15° scattering angle

for impact energies five–ten times transition energies (or, FBA and GOS are valid for $K^2 < 4 \text{ a.u.}^{-2}$). However we have found through comparisons to theory [96], as well as several tests of the impact energy independence of the derived GOS [87,92,95], that for inner shell excitation the GOS concept is valid to quite high momentum transfer. In the cases studied so far, this is true up to $K^2 < 40 \text{ a.u.}^{-2}$, or up to 40° scattering angle for impact energies which are more than five times the transition energy. The reason for this is not fully understood, but the more compact nature of the inner shell target may mean that the impact parameter [2,156] must be considerably smaller (and thus smaller impact energy, larger momentum transfer) before the interaction between the incident electron and the target becomes sufficiently strong that higher order terms in the Born expansion become appreciable.

Table 2 summarizes all of the studies reporting quantitative investigation of the angular dependence of *inner-shell* energy loss signals. A recent study of the GOS profiles for C 1s and O 1s excited CO₂ [96] illustrates this aspect of ISEELS. Fig. 9a compares C 1s ISEELS spectra of CO₂ recorded under dipole (4°) and non-dipole (32°) conditions. A linear background has been subtracted from each spectrum and the intensities are matched below 288 and above 320 eV in order to focus on changes in the spectral shape. This study was the first to locate the previously unknown ($2\sigma_g^{-1} 5\sigma_g^*$) $^1\Sigma_g$ state [157], which gives rise to the broad additional intensity between 298 and 302 eV in the 32° spectrum, which is not observed in the 4° spectrum (Fig. 9a). The experimental GOS profile for the broad C 1s ($2\sigma_g \rightarrow 5\sigma_g^*$) resonance centered at 298 eV is shown as Fig. 9b, the inset to Fig. 9a. The solid line is a polynomial Lassetre fit [2], used as a guide to the eye. The dipole forbidden character of this transition is evident from the extrapolation to zero GOS at $K^2 = 0$.

In this work the absolute GOS profiles for all resolved C 1s and O 1s electronic structures have been derived by careful consideration of all factors involved in relating the measured signals to the underlying differential cross-sections and the GOS [88,96]. For the discrete transitions, these have been compared to the GOS computed within the first Born approximation by Bielschowsky and Rocha [96]

Table 2

Summary of experimental and theoretical studies of generalized oscillator strengths for inner-shell excitation

Atom	Edge	Method	E_0 (eV)	Angle ($^\circ$)	E_n (eV)	Reference
Ar	Ar2p	E	4000	2–10	0–400	[164]
Kr	Kr3d,3p	E	3000	2–7	0–300	[164]
Ne	Ne 1s	E	2500	2–24	860–920	[104]
Xe	Xe4d	E	3000	1–11	0–150	[164]
		E	70–4000	1–20	70–200	[165]
<i>Molecule</i>						
CClF ₃	C 1s	E	2500	0.5–10	285–330	[159]
CCl ₂ F ₂	C 1s	E	2500	0.5–10	285–330	[159]
CCl ₃ F	C 1s	E	2500	0.5–10	285–330	[159]
CF ₄	C 1s	E	2500	0.5–10	285–330	[159]
COS	C 1s	E	1300	4–28	280–315	[160,161]
CO ₂	C 1s	E,T	1290	2–14	260–380	[107]
		T		0–15	290.7	[75]
		E	1300	4–36	285–330	[95]
CS ₂	C 1s	E	1300	4–28	280–310	[160,161]
C ₂ H ₂	C 1s	E,T	1290	2–18	280–292	[108]
CClF ₃	Cl 2p,2s	E	2500	0.5–10	195–240	[159]
CCl ₂ F ₂	Cl 2p,2s	E	2500	0.5–10	195–240	[159]
CCl ₃ F	Cl 2p,2s	E	2500	0.5–10	195–240	[159]
CCl ₄	Cl 2p,2s	E	2500	0.5–10	195–240	[159]
SF ₆	F 1s	E	1500	4–28	675–720	[88]
NO	N 1s	T		400		[101,102]
		E	3400	2–20	400	[103]
N ₂	N 1s	T			401	[101,102]
		E	1400/3400	2–20	401	[103]
		T			401	[74]
		E	25 000	10–100	150–650	[162,163]
N ₂ O	N 1s	T			400	[101,102]
		E	1400/3400	2–20	400	[103]
COS	O 1s	E	1300	4–20	520–560	[160,161]
CO ₂	O 1s	T		0–15	535.4	[75]
		E	1300	4–28	520–580	[95]
H ₂ O	O 1s	T	–	–	530–540	[77]
COS	S 2p,2s	E	1300	4–24	155–205	[160,161]
CS ₂	S 2p,2s	E	1300	4–28	160–185	[160,161]
SF ₆	S 2p,2s	E	2500	0.5–3.5	160–210	[106]
		E	1500	4–16	165–210	[91]
		E	1500	4–12	165–260	[93]
		E	1300	4–36	165–260	[88]

using rigorous ab initio codes, with large basis sets and configuration interaction. As an example, the experimental and computed GOS profiles for the C 1s ($2\sigma_g \rightarrow 2\pi_u^*$) transition are presented in Fig. 9c, in comparison to previously reported experimental [107] and computed values [75]. There is remarkably good agreement with the earlier experimental studies

(which used a different impact energy), as well as with theory, out to very large momentum transfer. This is evidence that the first Born approximation holds to a much larger momentum transfer in inner-shell than in valence electronic excitation. Fig. 9d compares the shape of the experimental GOS profile for the $4\sigma_u^*$ shape resonance to that for the non-

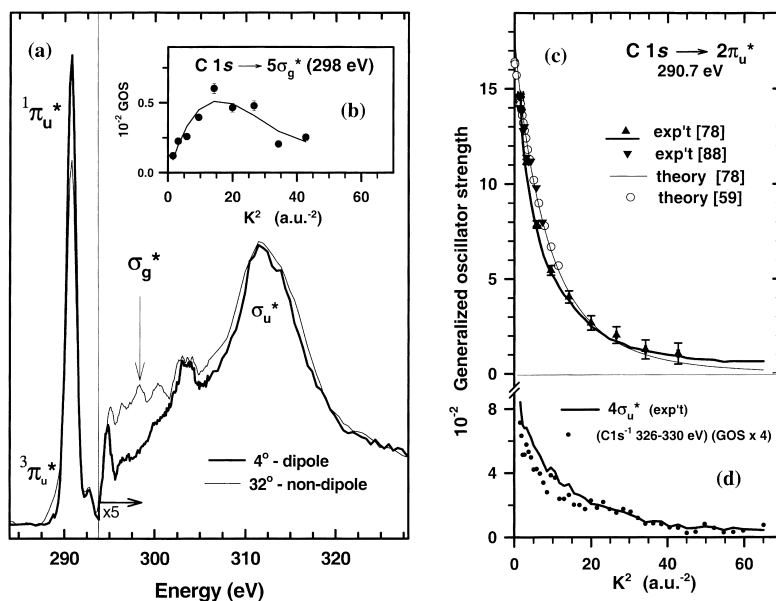


Fig. 9. (a) Comparison of dipole (4°) and non-dipole (32°) regime C 1s ISEELS of CO_2 recorded with a final electron energy of 1300 eV [96]. The intensities have been matched below 288 eV and above 320 eV. (b) [inset to (a)] Experimental GOS profile for the broad C 1s ($2\sigma_g \rightarrow 5\sigma_g^*$) resonance centered at 298 eV. The solid line is a polynomial Lassette fit, used as a guide to the eye. The dipole forbidden character of this transition is evident from the extrapolation to zero GOS at $K=0$. (c) Experimental and computed GOS profiles for the C 1s ($2\sigma_g \rightarrow 2\pi_u^*$) transition plotted in comparison to previously reported experimental [107] and computed values [75]. (d) Comparison of the shapes of experimental GOS profiles for the $4\sigma_u^*$ shape resonance (solid line) to that for the non-resonant C 1s continuum, integrated from 326 to 330 eV. The vertical scale is that for the GOS of the $4\sigma_u^*$ resonance. The GOS data for the non-resonant continuum signal has been multiplied $\times 4$. The deviation in shapes of these two GOS profiles indicates that shape resonances can affect inner shell ionization dynamics.

resonant C 1s continuum, integrated from 326 to 330 eV. Even at this level of statistical precision, it appears there is a difference in shape, with the GOS profile of the $4\sigma_u^*$ shape resonance being relatively less intense at large momentum transfer. While more accurate data is needed to confirm this result, the data so far suggests that the $4\sigma_u^*$ shape resonance may affect the dynamics of C 1s electron impact ionization. Shape resonances are well known to affect both electronic and nuclear motion in the time-evolution of electronic states [158]. Coupling between the excitation, time-evolution, and de-excitation would be required to explain a deviation of the GOS profiles for C 1s ionization in the region of the $4\sigma_u^*$ shape resonance. Since the time interval for interaction is larger at large momentum transfer relative to that at small momentum transfer [59], it is likely that the changes in GOS profile for the

resonant and non-resonant C 1s ionization occur in the high K^2 regime.

4. Summary and future trends

This review has presented a rather personal and perhaps eclectic perspective on the field of inner shell electron energy loss spectroscopy — its historical development and current themes. I apologize in advance to any of my colleagues who may consider their work under represented in the material I chose to discuss.

What are the prospects for the future? ISEELS has unique capabilities for non-dipole spectroscopy and spectrometry, significant advantages in deriving quantitative intensities and energies, and it is easier to adapt it to novel conditions such as chemical

reactions and high temperature operation than is often the case at a synchrotron. For these reasons, as well as the modest cost of the equipment, I believe the future for continued innovative and useful work in ISEELS is very good. One aspect which may have discouraged some researchers from entering this field, is the very weak signals involved. It is possible to measure dipole regime valence EELS at high energy resolution using current detection techniques but the cross-sections for inner-shell EELS are 100 to 1000 times smaller and thus counting techniques and careful minimization of systematic artifacts are extremely important. A common trend in electron spectroscopy at present is the adoption of parallel detection technology in electron spectrometers. We have recently implemented a two-dimensional, re-

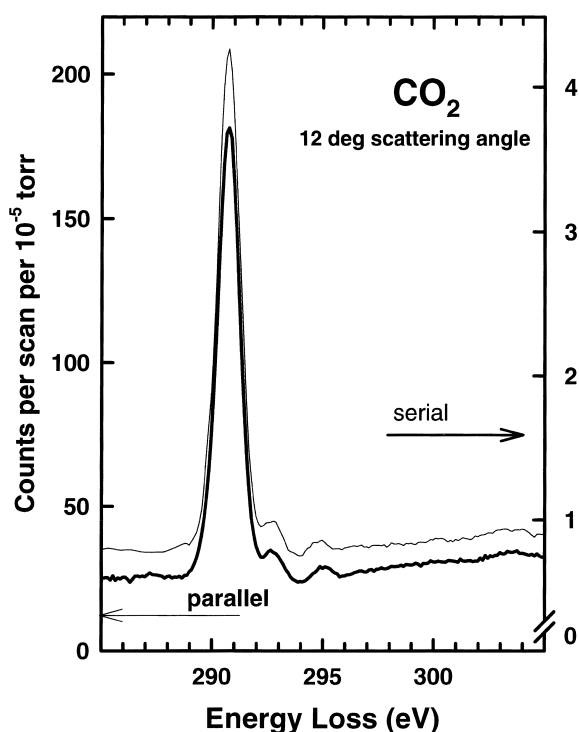


Fig. 10. C 1s ISEELS spectra of CO_2 recorded at 1500 eV impact energy, 0.5 eV fwhm energy resolution and 12° scattering angle with the parallel detector (left scale) and single channel serial detector (right scale). The accumulated signal has been normalized to incident current ($3 \mu\text{A}$ in each case), numbers of scans (four scans for parallel, 22 for serial, each scan being 2 min long) and the gas pressure (7×10^{-6} Torr for the parallel and 4×10^{-5} Torr for the serial measurement).

sistive anode, position sensitive detector [124] in McVAHRES. Fig. 10 is a direct comparison of the C 1s spectrum of CO_2 recorded at the same impact energy, energy resolution and scattering angle. The normalized signal acquisition rate is ~ 40 -fold higher with the parallel detector, an improvement in signal throughput that is consistent with the ratio of the widths of the dispersed spectrum sampled with the two detectors. In addition to faster acquisition which de-sensitizes the spectrometer to low frequency systematic noise, the 2-d detector [124] is a very powerful tool to assist spectrometer tuning since real-time imaging of the dispersed signal gives excellent insight into the peculiarities of electron optics and allows rapid and effective optimization of lens voltages. This data, which to my knowledge is the second published example of parallel detection ISEELS [112], was recorded with the unmonochromated mode. The large gain in signal acquisition rate will make practical many experiments in the monochromated mode which would have been extremely difficult or even impossible using a single channel detector. I look forward to the next 10 years of ISEELS as the instrumentation advances developed at McMaster and at other laboratories are exploited systematically.

Acknowledgements

The gas phase research program at McMaster University has been funded for many years by NSERC (Canada). The vision of this organization to provide funding for what is primarily fundamental, 'unfocussed' research is gratefully acknowledged. Additional financial support for gas phase studies has been provided by Dow Canada and Dow USA. I wish to thank research associate Tolek Tyliczszak who has made many key contributions to the instrumentation advances on both spectrometers, and to Stephen Urquhart, who provided the calculated spectra shown in Fig. 6. I acknowledge with thanks the contributions of all group members who have been associated with the gas phase experiments at McMaster: James Francis, Cassia Turci and Gabriella Eustatiu (McVAHRES); Tom Steel, Dave Newberry, Izumi Ishii, Steve Clark, Bruce Hollebhone, Alex Wen, Stephen Urquhart, John Lehmann, Laura

Ennis, Bob Lessard and Eiman Al-Hassan (ISEELS). The contributions of international colleagues in collaborative programs involving ISEELS are also acknowledged: Mel Robin, Eckart Rühl, John Gland, Peter Dowben, Ed Rightor and Nobuhiro Kosugi.

References

- [1] S. Trajmar, J.K. Rice, A. Kuppermann, in: L. Prigogine, S.A. Rice (Eds.), *Advanced Chemistry and Physics*, Vol. XVIII, Wiley, NY, 1970, p. 15.
- [2] R.A. Bonham, M. Fink, *High Energy Electron Scattering*, Reinhold, NY, 1974.
- [3] E.N. Lassette, A. Skerbele, *Meth. Exp. Phys.* 3B (1974) 868.
- [4] R.A. Bonham, in: C.R. Brundle, A.D. Baker (Eds.), *Electron Spectroscopy: Theory, Techniques and Applications*, Vol. 3, Academic, NY, 1979, p. 127.
- [5] C.E. Brion, A. Hamnett, in: J.W. McGowan (Ed.), *Advanced Chemistry and Physics*, Vol. 45.1, Wiley, BY, 1981.
- [6] W.H.E. Schwarz, *Angew. Chem. Int. Ed. Engl.* 13 (1974) 454.
- [7] J. Stöhr, *NEXAFS Spectroscopy*, Springer-Verlag, New York, 1992.
- [8] F.H. Read, *J. de Phys. Colloque (Paris)* 39 (1978) C1,C82.
- [9] C.E. Brion, S. Daviel, R.N.S. Sodhi, A.P. Hitchcock, *AIP Conf. Proc.* 94 (1982) 429.
- [10] A.P. Hitchcock, *Ultramicroscopy* 28 (1989) 165.
- [11] A.P. Hitchcock, *Physica Scripta* T31 (1990) 159.
- [12] A.P. Hitchcock, in: *Collision Processes of Ion, Positron, Electron and Photon Beams with Matter*, World Scientific Publishing, London, 1992, p. 104.
- [13] A.P. Hitchcock, D.C. Mancini, *J. Electron Spec. Relat. Phen.* 67 (1994) 1, Updates to Aug-98 are available upon request to the author, or by down load from unicorn.mcmaster.ca.
- [14] J.A. Prins, *Physica* 1 (1934) 1174.
- [15] M.J. Van der Wiel, Th.M. El-Sherbini, C.E. Brion, *Chem. Phys. Lett.* 7 (1970) 161.
- [16] J.W. Gallagher, C.E. Brion, J.A.R. Samson, P.W. Langhoff, *J. Phys. Chem. Ref. Data* 17 (1988) 9.
- [17] M.J. Van der Wiel, G. Wiebes, *Physica* 53 (1971) 225.
- [18] M.J. Van der Wiel, Th.M. El-Sherbini, *Physica* 59 (1972) 45.
- [19] R.B. Kay, Ph.E. van der Leeuw, M.J. Van der Wiel, *J. Phys.* B 10 (1977) 2512,2521.
- [20] A.P. Hitchcock, C.E. Brion, M.J. Van der Wiel, *J. Phys.* B 11 (1978) 3245.
- [21] A.P. Hitchcock, C.E. Brion, M.J. Van der Wiel, *Chem. Phys. Lett.* 66 (1979) 213.
- [22] G.R. Wight, C.E. Brion, *J. Electron Spectrosc.* 3 (1974) 191.
- [23] G.R. Wight, C.E. Brion, *J. Electron Spectrosc.* 4 (1974) 25.
- [24] G.R. Wight, C.E. Brion, *J. Electron Spectrosc.* 4 (1974) 313.
- [25] G.R. Wight, C.E. Brion, *J. Electron Spectrosc.* 4 (1974) 327.
- [26] G.R. Wight, C.E. Brion, *J. Electron Spectrosc.* 4 (1974) 335.
- [27] G.R. Wight, C.E. Brion, *J. Electron Spectrosc.* 4 (1974) 347.
- [28] G.R. Wight, C.E. Brion, *Chem. Phys. Lett.* 26 (1974) 607.
- [29] A.P. Hitchcock, C.E. Brion, *J. Electron Spectrosc.* 10 (1977) 31.
- [30] A.P. Hitchcock, C.E. Brion, *Chem. Phys.* 33 (1978) 55.
- [31] A.P. Hitchcock, C.E. Brion, *J. Electron Spectrosc.* 13 (1978) 193.
- [32] A.P. Hitchcock, C.E. Brion, *J. El. Spectrosc.* 14 (1978) 417.
- [33] A.P. Hitchcock, C.E. Brion, *J. El. Spectrosc.* 17 (1979) 139.
- [34] A.P. Hitchcock, M. Pocock, C.E. Brion, M.S. Banna, D.C. Frost, C.A. McDowell et al., *J. Electron Spectrosc.* 13 (1978) 345.
- [35] M. Tronc, G.C. King, R.C. Bradford, F.H. Read, *J. Phys.* B 9 (1976) L555.
- [36] G.C. King, J.W. McConkey, F.H. Read, *J. Phys.* B 10 (1977) L541.
- [37] G.C. King, M. Tronc, F.H. Read, R.C. Bradford, *J. Phys.* B 10 (1977) 2479.
- [38] G.C. King, F.H. Read, M. Tronc, *Chem. Phys. Lett.* 52 (1977) 50.
- [39] M. Tronc, G.C. King, F.H. Read, *J. Phys.* B 12 (1979) 137.
- [40] M. Tronc, G.C. King, F.H. Read, *J. Phys.* B 13 (1980) 999.
- [41] G.C. King, J.W. McConkey, F.H. Read, B. Dobson, *J. Phys.* B 13 (1980) 4315.
- [42] D.A. Shaw, G.C. King, F.H. Read, *J. Phys.* B 11 (1980) L723.
- [43] G.C. King, *Lecture Notes in Chemistry* 35 (1984) 162.
- [44] D.A. Shaw, D. Cvejanovic, G.C. King, F.H. Read, *J. Phys.* B 17 (1984) 1173.
- [45] D.A. Shaw, G.C. King, F.H. Read, D. Cvejanovic, *J. Phys.* B 15 (1982) 1785.
- [46] D.A. Shaw, G.C. King, D. Cvejanovic, F.H. Read, *J. Phys.* B 17 (1984) 2091.
- [47] D.A. Shaw, G.C. King, F.H. Read, *Chem. Phys. Lett.* 129 (1986) 17.
- [48] C.T. Chen, F. Sette, *Rev. Sci. Inst.* 60 (1989) 1616.
- [49] C.T. Chen, Y. Ma, F. Sette, *Phys. Rev. A* 40 (1989) 6737.
- [50] C.T. Chen, F. Sette, *Phys. Scripta.* T31 (1990) 119.
- [51] Y. Ma, C.T. Chen, G. Meigs, K. Randall, F. Sette, *Phys. Rev. A* 44 (1991) 1848.
- [52] M. Domke, C. Xue, A. Puschmann, T. Mandel, E. Hudson, D.A. Shirley et al., *Chem. Phys. Lett.* 173 (1990) 122.
- [53] M. Domke, T. Mandel, A. Puschmann, C. Xue, D.A. Shirley, G. Kaindl et al., *Rev. Sci. Inst.* 63 (1992) 80.
- [54] M. Domke, G. Remmers, G. Kaindl, *Nucl. Inst. Meth.* B 87 (1994) 173.
- [55] W. Butscher, R.J. Buenker, S.D. Peyerimhoff, *Chem. Phys. Lett.* 52 (1977) 449.
- [56] A. Barth, R.J. Buenker, S.D. Peyerimhoff, W. Butscher, *Chem. Phys.* 46 (1980) 149.
- [57] W.H.E. Schwarz, *Chem. Phys.* 11 (1975) 217.
- [58] W.H.E. Schwarz, *Chem. Phys.* 13 (1976) 153.
- [59] W.H.E. Schwarz, T.C. Chang, U. Seeger, K.H. Huang, *Chem. Phys.* 117 (1987) 73.
- [60] H. Köppel, F.X. Gadea, G. Klatt, J. Schirmer, L.S. Cederbaum, *J. Chem. Phys.* 106 (1997) 4415.
- [61] J. Schirmer, A. Barth, F. Tarantelli, *Chem. Phys.* 122 (1988) 9.

- [62] L. Yang, H. Ågren, *Phys. Rev. B* 54 (1996) 1.
- [63] H. Ågren, L. Yang, V. Carravetta, L.G.M. Pettersson, *Chem. Phys. Lett.* 259 (1996) 21.
- [64] L. Yang, H. Ågren, L.G.M. Pettersson, V. Carravetta, *J. Electron Spectrosc.* 83 (1997) 209.
- [65] N. Kosugi, H. Kuroda, *Chem. Phys. Lett.* 74 (1980) 490.
- [66] N. Kosugi, *Theor. Chim. Acta.* 72 (1987) 149.
- [67] N. Kosugi, *J. Electron Spectrosc.* 79 (1996) 351.
- [68] E. Rühl, A.P. Hitchcock, *J. Am. Chem. Soc.* 111 (1989) 5069.
- [69] E. Rühl, A.T. Wen, A.P. Hitchcock, *J. Electron Spectrosc.* 57 (1991) 137.
- [70] J.T. Francis, A.P. Hitchcock, *J. Phys. Chem.* 98 (1994) 3650.
- [71] C. Mealli, D.M. Proserpio, *J. Chem. Ed.* 67 (1990) 399, The Huckel code and visualization program Computer Aided Composition of Atomic Orbitals (CACAO) is freeware available from Proserpio by anonymous ftp (cacao.isseccfi.cnr.it) or via Web download (e.g. <http://www.ccl.net/ccs/documents/chamotlabs/SoftWare.shtml>).
- [72] C.H. Hu, D.P. Chong, *Chem. Phys. Lett.* 262 (1996) 729.
- [73] D.P. Chong, C.H. Hu, *J. Electron Spectrosc.* 24 (1998) 181.
- [74] C.E. Bielschowsky, M.A.C. Nascimento, B. Hollauer, *Phys. Rev. A* 45 (1992) 7942.
- [75] M.P. de Miranda, C.E. Bielschowsky, *J. Mol. Struct. (Theochem)* 282 (1993) 71.
- [76] M.P. de Miranda, C.E. Bielschowsky, M.A.C. Nascimento, *J. Phys. B* 28 (1995) L15.
- [77] A.B. Rocha, C.E. Bielschowsky, *Chem. Phys.* 243 (1999) 9.
- [78] L. Ungier, T.D. Thomas, *Chem. Phys. Lett.* 96 (1983) 247.
- [79] L. Ungier, T.D. Thomas, *Phys. Rev. Lett.* 53 (1984) 435.
- [80] L. Ungier, T.D. Thomas, *J. Chem. Phys.* 82 (1985) 3146.
- [81] T.X. Carroll, S.E. Anderson, L. Ungier, T.D. Thomas, *Phys. Rev. Lett.* 58 (1987) 867.
- [82] T.X. Carroll, T.D. Thomas, *J. Chem. Phys.* 89 (1988) 5983.
- [83] S. Daviel, C.E. Brion, A.P. Hitchcock, *Rev. Sci. Inst.* 55 (1984) 182.
- [84] I. Harrison, G.C. King, *J. Phys. B* 19 (1986) L447.
- [85] I. Harrison, G.C. King, *J. Electron Spectrosc.* 43 (1987) 155.
- [86] I. Harrison, G.C. King, L. Avaldi, *J. Phys. B* 21 (1988) 4015.
- [87] J.T. Francis, PhD Thesis, McMaster, 1995.
- [88] I.G. Eustatiu, J.T. Francis, T. Tylliszczak, C.C. Turci, A.L.D. Kilcoyne, A.P. Hitchcock, *Chem. Phys.* 275 (2000) 235.
- [89] J.T. Francis, C. Enkvist, S. Lunell, A.P. Hitchcock, *Can. J. Phys.* 72 (1994) 879.
- [90] J.T. Francis, N. Kosugi, A.P. Hitchcock, *J. Chem. Phys.* 101 (1994) 10429.
- [91] J.T. Francis, C.C. Turci, T. Tylliszczak, G.G.B. de Souza, N. Kosugi, A.P. Hitchcock, *Phys. Rev. A* 52 (1995) 4665.
- [92] C.C. Turci, J.T. Francis, T. Tylliszczak, G.G.B. de Souza, A.P. Hitchcock, *Phys. Rev. A* 52 (1995) 4678.
- [93] A.P. Hitchcock, I.G. Eustatiu, J.T. Francis, C.C. Turci, *J. Electron Spectrosc.* 88–91 (1998) 77.
- [94] I.G. Eustatiu, B. Huo, S.G. Urquhart, A.P. Hitchcock, *J. Electron Spectrosc.* 94 (1998) 243.
- [95] I.G. Eustatiu, T. Tylliszczak, A.P. Hitchcock, *Chem. Phys. Lett.* 300 (1999) 676.
- [96] I.G. Eustatiu, T. Tylliszczak, A.P. Hitchcock, C.C. Turci, A.B. Rocha, C.E. Bielschowsky, *Phys. Rev. A* 61 (2000) 042505.
- [97] H.H. Wellenstein, R.A. Bonham, *Chem. Phys. Lett.* 15 (1972) 530.
- [98] H.F. Wellenstein, H. Schmoranzler, R.A. Bonham, T.C. Wong, J.S. Lee, *Rev. Sci. Inst.* 46 (1975) 92.
- [99] A.L. Bennani, H.F. Wellenstein, A. Diguët, B. Nguyen, A.D. Barlas, *Chem. Phys. Lett.* 41 (1976) 470.
- [100] A.L. Bennani, A. Diguët, H.F. Wellenstein, *Chem. Phys. Lett.* 60 (1979) 405.
- [101] R. Camilloni, B. Fainelli, G. Petracelli, G. Stefani, F. Moracci, R. Platania, *Lecture Notes in Chemistry* 35 (1984) 172.
- [102] R. Camilloni, B. Fainelli, G. Petracelli, G. Stefani, *J. Phys. B* 20 (1987) 1839.
- [103] L. Avaldi, R. Camilloni, G. Stefani, *Phys. Rev. A* 41 (1990) 134.
- [104] C.D. Schröter, L. Avaldi, R. Camilloni, G. Stefani, M. Zitnik, M. Stuehec, *J. Phys. B* 32 (1999) 171.
- [105] J.F. Ying, K.T. Leung, *J. Chem. Phys.* 101 (1994) 7311.
- [106] J.F. Ying, C.P. Mathus, K.T. Leung, *Phys. Rev. A* 47 (1993) R5.
- [107] H.M. Boechat-Roberly, C.E. Bielschowsky, G.G.B. de Souza, *Phys. Rev. A* 44 (1991) 1694.
- [108] M.P. de Miranda, C.E. Bielschowsky, H.M. Boechat-Roberly, G.G.B. de Souza, *Phys. Rev. A* 49 (1994) 2399.
- [109] J.C. Giordan, J.H. Moore, J.A. Tossell, *J. Am. Chem. Soc.* 107 (1985) 5600.
- [110] A. Benitez, J.H. Moore, J.A. Tossell, *J. Chem. Phys.* 88 (1988) 6691.
- [111] X. Wan, J.H. Moore, J.A.I. Tossell, *Chem. Phys.* 21 (1989) 7343.
- [112] C. Hannay, J. Heinesch, U. Kleyens, M.J. Hubin-Franskin, *Meas. Sci. Tech.* 6 (1995) 1140.
- [113] M.J. Hubin-Franskin, H. Aouni, D. Duflot, F. Motte-Tollet, C. Hannay, L.F. Ferreira, G. Tourillion, *J. Chem. Phys.* 106 (1997) 35.
- [114] D. Duflot, C. Hannay, J.P. Flament, M.J. Hubin-Franskin, *J. Chem. Phys.* 109 (1998) 5308.
- [115] C. Hannay, D. Duflot, J.P. Flament, M.J. Hubin-Franskin, *J. Chem. Phys.* 110 (1999) 5600.
- [116] L. Kerwin, P. Marmet, J.D. Carette, in: E.W. McDaniel, M.R.C. McDowell (Eds.), *Case Studies in Atomic Collision Physics I*, North-Holland, Amsterdam, 1969, p. 526.
- [117] C.E. Brion, *M.T.P. Int. Rev. Sci.* 5 (1971) 55.
- [118] B. Harting, F.H. Read, *Electrostatic Lenses*, Elsevier, Amsterdam, 1976.
- [119] F.H. Read and N. Bowering, RB Consultants Ltd., UK Registered Company #2813339.
- [120] A. Chutjian, *J. Chem. Phys.* 61 (1974) 4279.
- [121] C.E. Kuyatt, J.A. Simpson, *Rev. Sci. Inst.* 38 (1967) 103.
- [122] C.E. Kuyatt, *Lecture Notes on Electron Optics* (1967) unpublished.
- [123] P. Grivet, *Electron Optics*, second ed, Pergamon, Oxford, 1972.
- [124] Quantar Technology Inc., Santa Cruz, CA, 95060.
- [125] L.E. Ennis, A.P. Hitchcock, *J. Chem. Phys.* 111 (1999) 3468.

- [126] W.F. Chan, G. Cooper, C.E. Brion, *Phys. Rev. A* 44 (1991) 186.
- [127] T.R. Olney, N.M. Cann, G. Cooper, C.E. Brion, *Chem. Phys.* 223 (1997) 59.
- [128] T. R. Olney, C.E. Brion, T. Ibuki, *Chem. Phys.* 201 (1996) 505.
- [129] R.N.S. Sodhi, C.E. Brion, *J. Electron Spectrosc.* 34 (1984) 363.
- [130] R. McLaren, I. Ishii, A.P. Hitchcock, M.B. Robin, *J. Chem. Phys.* 201 (1987) 4344.
- [131] B.L. Henke, E.M. Gullikson, J.C. Davis, *Data Nucl. Data Tables* 54 (1993) 181, Atomic constants available from http://www-cxro.lbl.gov/optical_constants/.
- [132] C.C. Turci, S.G. Urquhart, A.P. Hitchcock, *Can. J. Chem.* 74 (1996) 851.
- [133] W. Domcke, L.S. Cederbaum, J. Schirmer, W. von Niessen, *Phys. Rev. Lett.* 42 (1979) 1237.
- [134] S.G. Urquhart, A.P. Hitchcock, A.P. Smith, H. Ade, E.G. Rightor, *J. Phys. Chem. B* 101 (1997) 2267.
- [135] I.G. Eustatiu, B. Huo, S.G. Urquhart, A.P. Hitchcock, *J. Electron Spectrosc.* 94 (1998) 24.
- [136] A.P. Hitchcock, G. Tourillon, W. Braun, *Can. J. Chem.* 67 (1989) 1819.
- [137] A.P. Hitchcock, G.P. Williams, R. Garrett, G. Tourillon, *J. Phys. Chem.* 93 (1989) 7624.
- [138] A.P. Hitchcock, G. Tourillon, R. Garrett, G.P. Williams, C. Mahatsekake, C. Andrieu, *J. Phys. Chem.* 94 (1990) 2327.
- [139] A.P. Hitchcock, S.G. Urquhart, E.G. Rightor, *J. Phys. Chem.* 96 (1992) 8736.
- [140] S.G. Urquhart, A.P. Hitchcock, R.D. Leapman, R.D. Pries-ter, E.G. Rightor, *J. Polym. Sci. B: Polym. Phys.* 33 (1995) 1593,1603.
- [141] E.G. Rightor, A.P. Hitchcock, H. Ade, R.D. Leapman, S.G. Urquhart, A.P. Smith et al., *J. Phys. Chem. B* 101 (1997) 1950.
- [142] S.G. Urquhart, A.P. Hitchcock, A.P. Smith, H. Ade, W. Lidy, E.G. Rightor et al., *J. Electron Spectrosc. Rel. Phenom.* 100 (1999) 119.
- [143] H. Ade, S.G. Urquhart, in: T.K. Sham (Ed.), *Chemical Applications of Synchrotron Radiation*, Advanced Series of Physical Chemistry, World Scientific, Singapore, 2000.
- [144] J.A. Horsley, J. Stöhr, A.P. Hitchcock, D.C. Newbury, A.L. Johnson, F. Sette, *J. Chem. Phys.* 83 (1985) 6099.
- [145] I. Ishii, A.P. Hitchcock, *J. Chem. Phys.* 87 (1987) 830.
- [146] I. Ishii, A.P. Hitchcock, *J. Electron Spectrosc.* 46 (1987) 55.
- [147] D.A. Outka, J. Stöhr, R.J. Madix, R.R. Rotermund, B. Hermsmeier, J. Solomon, *Surf. Sci.* 185 (1987) 53.
- [148] B. Hirota, *High Resolution Spectroscopy of Transient Molecules*, Springer-Verlag, New York, 1985.
- [149] J.M. Dyke (Ed.), *J. El. Spec. Relat. Phen* 97 (1998), Special issue on photoelectron spectroscopy of transients.
- [150] S.G. Urquhart, A.P. Hitchcock, J.F. Lehmann, M. Denk, *Organometallics* 17 (1998) 2352.
- [151] J.F. Lehmann, L. Ennis, A.P. Hitchcock, S.G. Urquhart, K. Hatano, S. Gupta, M.K. Denk, *Organometallics* 18 (1999) 1862.
- [152] M. Denk, R. Lennon, R. Hayashi, R. West, A.V. Belyakov, H.P. Verne, A. Haaland, M. Wagner, N. Metzler, *J. Am. Chem. Soc.* 116 (1994) 2691.
- [153] J.F. Lehmann, B.Sc. Thesis, McMaster, 1998.
- [154] H.W. Kroto, R.J. Suffolk, N.P.C. Westwood, *Chem. Phys. Lett.* 22 (1973) 495.
- [155] T.P. Fehlner, D.W. Turner, *J. Am. Chem. Soc.* 95 (1973) 7175.
- [156] M. Inokuti, *Rev. Mod. Phys.* 43 (1971) 297.
- [157] J. Stöhr, *J. Chem. Phys.* 87 (1987) 3523.
- [158] S. Sundin, A. Ausmees, O. Bjornholm, S.L. Sorensen, M. Wiklund, A. Kikas et al., *Phys. Rev. A* 58 (1998) 2037.
- [159] J.F. Ying, C.P. Mathers, K.T. Leung, *Phys. Rev. A* 101 (1994) 7311.
- [160] I.G. Eustatiu, McMaster PhD Thesis, 2000.
- [161] C.C. Turci, I.G. Eustatiu, A.B. Rocha, C.E. Bielschowsky, A.P. Hitchcock, to be published.
- [162] R.A. Bonham, M. Inokuti, R.S. Barbieri, *J. Phys. B* 26 (1973) 3363.
- [163] R.S. Barbieri, R.A. Bonham, *Phys. Rev. A* 4 (1992) 7929.
- [164] V.C. Afrosimov, Yu.S. Gordeev, S.G. Lavrov, Y.M. Shelenin, *Soy. Phys. JETP* 28 (1969) 821.
- [165] M. Byong-Soo, Y. Yoshinari, T. Watabe, Y. Tanaka, C. Takayanagi, T. Takayanagi, K. Wakiya, H. Suzuki, *J. Phys. Soc. Jpn.* 62 (1993) 1183.